RSC Advances

PAPER

View Article Online
View Journal | View Issue

Cite this: *RSC Adv.*, 2016, **6**, 19389

Dispersion stability of chemically reduced graphene oxide nanoribbons in organic solvents†

Min Yeong Song,‡ Young Soo Yun,‡ Na Rae Kim and Hyoung-Joon Jin*

Received 11th November 2015
Accepted 8th February 2016

DOI: 10.1039/c5ra23801c

www.rsc.org/advances

In this study, the dispersion stability of graphene oxide nanoribbons (GONRs) and chemically reduced GONRs (CR-GONRs) in various organic solvents was investigated. Homogeneous colloidal suspensions of GONRs were obtained in hydrophilic solvents such as water, *N*,*N*-dimethylformamide (DMF), and *N*-methyl-2-pyrrolidone (NMP). After chemical reduction, amphiphilic dispersion behaviour of CR-GONRs was observed over a wide range of solvents including water, methanol, ethanol, DMF, NMP, acetone, styrene, and xylene. In contrast, the dispersion stability of CR-GONRs was poor in ambiguously hydrophilic or hydrophobic solvents such as tetrahydrofuran, methyl methacrylate, and chloroform.

Introduction

Nanostructured sp^2 carbon allotropes, such as fullerene, carbon nanotubes (CNTs), and graphene, have attracted considerable attention in numerous scientific fields over the last few decades. These allotropes have applications in electronics,[1–4] optics,[5–7] energy storage/conversion,[8–12] catalysis,[13–15] polymer composites,[16–21] actuators,[22,23] and sensing[24,25] because of their unusual properties and nanometre-scale effects. Graphene nanoribbons, one type of nanostructured sp^2 carbon allotrope, are ultra-thin strips of graphene containing numerous edge/defect sites with outstanding electronic and spin transport properties.[26–28] Recently, Kosynkin *et al.* reported the longitudinal unzipping of CNTs to form graphene nanoribbons.[29] This provides a relatively easy method for the production of large amounts of graphene oxide nanoribbons (GONRs), and a similar reduction protocol to that of graphene oxide (GO) can be applied to restore the damaged properties of GONRs.[29] Reduced GONRs are expected to have unique characteristics, distinct from those of CNTs and graphene. However, the main obstacle to their use is the homogeneous dispersion in organic solvents. These nanomaterials have a high surface energy, inducing aggregation during wet processes.[30] Although surface modification of GONRs can lead to stable dispersions in specific solvents, these methods are complex. Hence, it would be preferable if the reduced GONRs could be used directly without any surface modification and special techniques.

In a previous study, Park *et al.* reported the colloidal suspension of chemically reduced GOs over a wide range of organic solvents, from hydrophilic ethanol to hydrophobic tetrahydrofuran.[31] This simple dispersion method required no further chemical treatment besides reduction using hydrazine. Considering the morphological and structural differences between GONRs and GOs, their dispersion behaviours may vary. Further studies are required for practical applications of GONRs. However, to the best of our knowledge, the dispersion behaviour of GONRs has not yet been reported.

In this study, GONRs and chemically reduced GONRs (CR-GONRs) were prepared by unzipping CNTs, followed by a hydrazine reduction treatment. The dispersion behaviours of GONRs and CR-GONRs in various organic solvents were investigated.

Experimental section

Preparation of GONRs

GONRs were prepared according to a previously reported method.[29] Briefly, 150 mg of multi-walled CNTs (MWCNTs, 95%, Hanwha Nanotech Inc., Korea) were treated in concentrated sulfuric acid for 12 h, and 750 mg of $KMnO_4$ were added into the solution. The reaction mixture was stirred at room temperature for 1 h, and then heated to 55–70 °C for an additional 1 h. The reaction mixture was poured into 400 mL of ice containing 50 mL of 30% H_2O_2. The solution was filtered using a polytetrafluoroethylene membrane, and washed with distilled water. The obtained GONRs were dispersed in distilled water and frozen at −196 °C. The samples were then freeze-dried at −50 °C and 0.0045 mbar for 72 h. The resulting GONRs were stored in a vacuum oven at 30 °C.

Observation of GONR dispersion behaviour

Dried GONRs (0.01 wt%) were ultrasonicated (power and frequency of 200 W and 20 kHz, respectively) in water, methanol (MeOH), ethanol (EtOH), *N*,*N*-dimethylformamide (DMF),

Department of Polymer Science and Engineering, Inha University, Incheon 402-751, South Korea. E-mail: hjjin@inha.ac.kr

† Electronic supplementary information (ESI) available. See DOI: 10.1039/c5ra23801c

‡ These authors contributed equally to this work.

N-methyl-2-pyrrolidone (NMP), acetone, tetrahydrofuran (THF), methyl methacrylate (MMA), chloroform, styrene, xylene, toluene, and hexane for 10 min. The dispersion behaviour of GONRs in these solvents was observed for 24 h. The dispersion behaviour of GONRs was further investigated in mixed solvent systems, such as (water, DMF, NMP)/(MeOH, EtOH, acetone, THF, MMA, chloroform, styrene, xylene, toluene, hexane). The mixed solvent systems were prepared by adding 2 g of 0.1 wt% GONRs dispersed in water, DMF, and NMP into 18 g of MeOH, EtOH, acetone, THF, MMA, chloroform, styrene, xylene, toluene, and hexane.

Preparation of homogeneous CR-GONR dispersions

GONRs (0.1 wt%) were ultrasonicated in water, DMF, NMP, water/MeOH, water/EtOH, and water/acetone for 10 min. The homogeneous GONR dispersions (20 g) were heated at 90 °C, before 100 μL of hydrazine were added. Reaction mixtures were stirred at 90 °C for 12 h. After chemical reduction with hydrazine, CR-GONR dispersions in solvents were obtained.

Observation of CR-GONR dispersion behaviour

Homogeneous colloidal suspensions of CR-GONRs in DMF (0.1 wt%) were added into solvents, such as water, methanol, ethanol, NMP, acetone, THF, MMA, chloroform, styrene, xylene, toluene, and hexane, with a DMF : solvent ratio of 1 : 9 (wt ratio). As a result, 0.01 wt% CR-GONR dispersions were obtained in various solvents. The dispersion behaviour of CR-GONRs in various solvents was observed for 24 h.

Characterization

The morphology of the samples was examined using field-emission scanning electron microscopy (FE-SEM, S-4300, Hitachi, Tokyo, Japan) and field-emission transmission electron microscopy (FE-TEM, JEM2100F, JEOL, Tokyo, Japan). The Raman spectra were recorded using a continuous-wave linearly polarized laser (wavelength, excitation energy, and power of 514.5 nm, 2.41 eV, and 16 mW, respectively). The laser beam was focused using a 100× objective lens, resulting in a spot diameter of approximately 1 μm. The acquisition time and number of circulations to collect each spectrum were 10 s and three, respectively. X-ray diffraction (XRD, Rigaku DMAX 2500) was performed using a Cu-Kα radiation (wavelength λ = 0.154 nm) operated at 40 kV and 100 mA. The chemical composition of the samples was examined by X-ray photoelectron spectroscopy (XPS, PHI 5700 ESCA, Chanhassen, MN, USA) with a monochromatic Al-Kα radiation ($h\nu$ = 1486.6 eV). The dispersion behaviour of GONRs was characterized in detail using a Turbiscan® instrument (Formulaction, France), operating at a wavelength of 880 nm.

Results and discussion

GONRs were prepared from MWCNTs with a diameter of approximately 20 nm and length of several micrometres, as shown in Fig. S1.† The morphology of GONRs was studied by FE-TEM and FE-SEM [Fig. 1(a)–(d)]. Numerous GONRs were entangled with each other on a holey grid [Fig. 1(a) and (b)]. The high-resolution TEM image showed that GONRs had a nanometre-scale thickness and an amorphous carbon structure without long-range ordering [Fig. 1(c)]. The Raman spectrum of GONRs showed distinct D and G bands at approximately 1350 and 1580 cm^{-1}, respectively [Fig. 1(e)]. These bands correspond to the disorder in the A_{1g} breathing mode of the six-fold aromatic ring near the basal structure, and the hexagon structure related to the E_{2g} vibration mode of the sp^2-hybridised C atoms, respectively.[32]

The I_D/I_G intensity ratio of GONRs was approximately 0.89, indicating a hexagonal carbon structure of a few nanometres in size. The XRD pattern of GONRs shows broad graphitic (002) and (100) peaks [Fig. 1(f)], indicating an amorphous carbon structure composed of few layer graphene. The broad XRD pattern of GONRs is also distinct from that of MWCNTs [Fig. S1(f)†], resulting from their unzipping and exfoliation. The surface properties of GONRs were investigated by XPS [Fig. 2(a) and (b)]. In the XPS C 1s spectrum, three distinct peaks were observed: a main C–C bonding centred at 284.7 eV, and two C–O and C=O bonds centred at 286.9 and 288.7 eV, respectively [Fig. 2(a)].[33] The XPS O 1s spectrum shows two C–O and C=O bonds centred at 532.7 eV and 531.8 eV, respectively [Fig. 2(b)].[34] The C/O ratio was 2.3, indicating that numerous oxygen groups were present on the surface of GONRs.

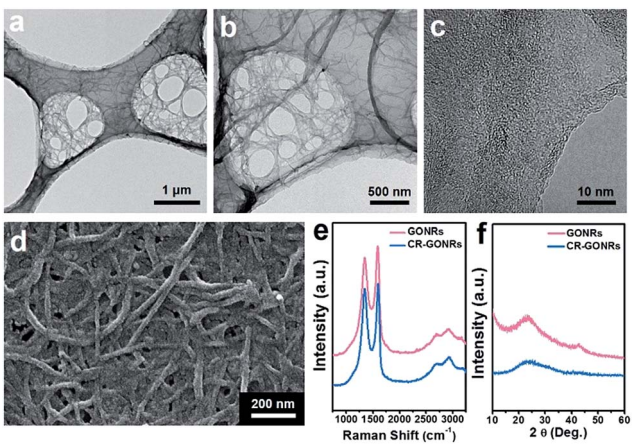

Fig. 1 (a)–(c) FE-TEM images of GONRs under different magnifications. (d) FE-SEM image of GONRs. (e) Raman spectra of GONRs (pink) and CR-GONRs (blue). (f) XRD patterns of GONRs (pink) and CR-GONRs (blue).

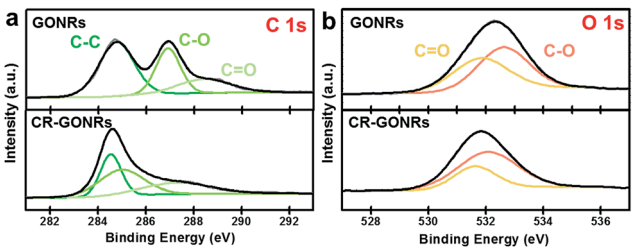

Fig. 2 XPS (a) C 1s, and (b) O 1s spectra of GONRs and CR-GONRs.

The dispersion stability of GONRs was studied in various organic solvents, including protic (water, MeOH, and EtOH), aprotic polar (DMF, NMP, acetone, and THF) and nonpolar (chloroform, xylene and toluene), and liquid monomers (MMA and styrene), as shown in Table 1 and Fig. 3. Highly stable colloidal suspensions of 0.01 wt% GONRs were obtained in water, DMF, and NMP [Fig. 3]. Moreover, no sedimentation was observed even after three months [Fig. S2†]. These solvents all have high surface tensions ($\gamma \geq 37.10$ mJ m^{-2}) and hydrophilic properties ($\delta_p + \delta_h \geq 19.5$ MPa$^{1/2}$) [Table 1]. In contrast, nonpolar solvents, liquid monomers, and some polar solvents (acetone and THF) resulted in a poor dispersion stability of 0.01 wt% GONRs. The GONRs also showed poor dispersion stabilities in protic solvents, such as EtOH and MeOH, with high $\delta_p + \delta_h$ values of 28.2 MPa$^{1/2}$ and 34.6 MPa$^{1/2}$, respectively, suggesting that several factors affect the dispersion behaviour of GONRs, in addition to hydrophilicity. An homogeneous colloidal suspension indicates that mixing between GONRs and organic solvents has a negative ΔG_{mix}. Because the entropy of mixing, calculated using Flory's equation, is very small compared to that obtained by the equation $\Delta H_{mix} < T\Delta S_{mix}$, ΔH_{mix} could be extremely small or negative.[35] The enthalpy of mixing depends on the balance between GONRs and the solvent surface energy, as shown in the following equation:[36]

$$\frac{\Delta H_{mix}}{V_{mix}} \approx \frac{2}{T_G}(\delta_G - \delta_{sol})^2 \phi, \quad (1)$$

where $\delta_i = \sqrt{E_{sur}{}^i}$ is the square root of the surface energy of phase i, T_G is the thickness of GONRs, and ϕ is the volume fraction of GONRs. Therefore, in order to achieve a stable colloidal suspension over a wide range of solvents, GONRs have to contain various chemical structures with different surface energies. Additionally, good solvent mixtures (1 : 9 wt ratio) such as MeOH/water and EtOH/water show stable dispersion behaviours over a few days [Fig. 4]. The dispersion stability of binary MeOH/water and EtOH/water mixtures could be obtained by an increase of the surface tension. This result suggests a tuning potential for the dispersion behaviour of GONRs using binary solvent systems. The stable GONRs suspensions in water, DMF, NMP, and mixed solvents were used for chemical reduction with hydrazine. In the mixed solvents, GONRs flocculated a few minutes after adding hydrazine into the suspensions. This indicates that an intermediate structure between GONRs and CR-GONRs is not stable in mixed solvents.

Table 1 Hansen solubility parameters (in MPa$^{1/2}$) and surface tension (in mJ m^{-2} at 20 °C) for different organic solvents, and corresponding dispersion stabilities of GONRs and CR-GONRs

Solvent	δ_p	δ_h	$\delta_p + \delta_h$	γ	GONRs[a]	CR-GONRs[a]
Water	16	42.3	58.3	72.80	+++++	+++++
MeOH	12.3	22.3	34.6	22.70	+	+++++
EtOH	8.8	19.4	28.2	22.10	+	+++++
DMF	13.7	11.3	25	37.10	+++++	+++++
NMP	12.3	7.2	19.5	40.79	+++++	+++++
Acetone	10.4	7	17.4	25.2	–	+++++
THF	5.7	8	13.7	26.40	–	++
MMA	6.5	5.4	11.9	28.00	–	++
Chloroform	3.1	5.7	8.8	27.50	–	+
Styrene	1.0	4.1	5.1	32.14	–	+++++
Xylene	1.0	3.1	4.1	28.90	–	+++++
Toluene	1.4	2	3.4	28.40	–	+++
Hexane	0	0	0	18.43	–	Immiscible

[a] –, +, ++, +++, ++++, and +++++ indicate dispersion stabilities for 0 min, 1 min, 30 min, 1 h, 6 h, and 24 h.

Fig. 3 Photograph of 0.01 wt% GONRs dispersions in various organic solvents 24 h after the ultrasonication treatment (from left: water, methanol, ethanol, DMF, NMP, acetone, THF, MMA, chloroform, styrene, xylene, toluene, hexane).

Suspensions seem to be stable for several hours in water. However, agglomerates were eventually observed after chemical reduction. In contrast, homogeneous suspensions were maintained during the overall reduction process using DMF and NMP, and high concentration suspensions of approximately 2 mg mL^{-1} were obtained. The schematic representation of GONRs dispersion behaviour and chemical reduction process is depicted in Fig. S3.†

The chemical structure of CR-GONRs was investigated by XPS. The XPS C 1s spectrum of CR-GONRs showed that the C–O bonding centred at 285.0 eV decreased considerably, and the C–C bonding centred at 284.5 eV became narrower than that of GONRs. This indicates the removal of oxygen functional groups and partial restoration of the sp^2 carbon lattice [Fig. 2]. The C/O ratio of CR-GONRs was 3.2, indicating the existence of numerous oxygen functional groups. In the XPS O 1s spectrum, a similar ratio between C–O and C=O bonding was revealed [Fig. 2]. Despite the changes in chemical structure, the Raman

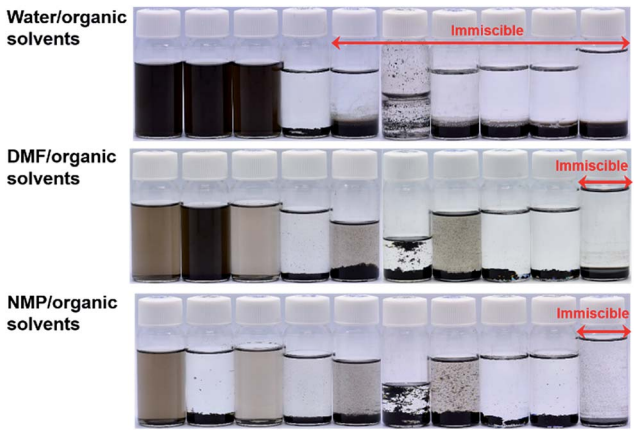

Fig. 4 Photograph of 0.01 wt% GONRs dispersions in water, DMF, and NMP/organic solvent (from left: methanol, ethanol, acetone, THF, MMA, chloroform, styrene, xylene, toluene, hexane) three days after ultrasonication.

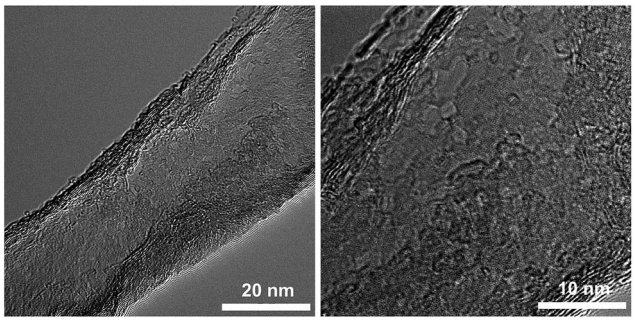

Fig. 5 High-resolution TEM images of CR-GONRs under different magnifications.

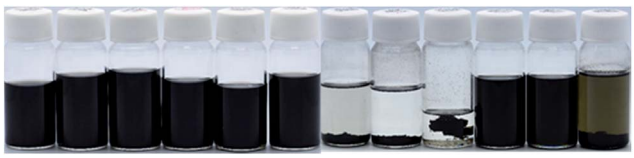

Fig. 6 Photograph of 0.01 wt% CR-GONRs dispersions 24 h after the ultrasonication treatment in various organic solvents (from left: water, methanol, ethanol, DMF, NMP, acetone, THF, MMA, chloroform, styrene, xylene, toluene).

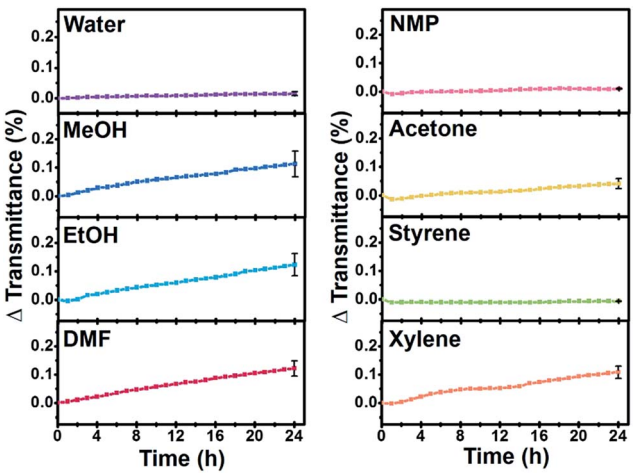

Fig. 7 Time *vs.* transmittance variation plot of 0.01 wt% CR-GONRs suspensions in various organic solvents obtained from Turbiscan®.

spectrum and XRD pattern of CR-GONRs are similar to those of GONRs, indicating that the hexagonal carbon structure and stacked graphene layers are a few nanometres in size. The high-resolution TEM micrograph shows that CR-GONRs have a highly defective carbon structure that contains various hole-cluster defects, topological defects, and numerous edge sites (Fig. 5). These complex structures could lead to different surface energies, affecting the dispersion behaviour of CR-GONRs.

The dispersion stability of CR-GONRs in organic solvents was investigated by adding a 0.1 wt% CR-GONRs/DMF suspension into various organic solvents with a 1 : 9 weight ratio. The final concentrations of CR-GONRs were controlled at 0.01 wt%. As shown in Fig. 6, stable colloidal suspensions were obtained over a wide range of solvents, including water, MeOH, EtOH, DMF, NMP, acetone, styrene, and xylene. This result indicated that chemical reduction led to a dramatic change in the dispersibility of GONRs. Interestingly, the dispersion stability of CR-GONRs extended into both hydrophobic and hydrophilic solvents. In contrast, CR-GONRs showed poor dispersibility in THF, MMA, and chloroform, which have intermediate $\delta_p + \delta_h$ values (between 8.8 and 13.7 $MPa^{1/2}$). The amphiphilic dispersion behaviour of CR-GONRs suggests that a complex chemical structure including oxygen functional groups, topological defect clusters, pseudo-edge sites of hole-cluster defects in the basal plane, and edge/defect sites work individually to form stable dispersions. The dispersion stability of the best solvents was characterized in detail using a Turbiscan® instrument,[37] where transmittance variation *versus* time provided quantitative dispersion stability measurements for CR-GONRs (Fig. 7). CR-GONRs suspensions showed no transmittance variation after 24 h in water, NMP, and styrene, whereas only a small transmittance variation of approximately 0.12% was observed in EtOH, MeOH, DMF, and xylene. This confirms that CR-GONRs have a good dispersion stability in various organic solvents. Additionally, we performed zeta potential measurements for CR-GONRs in several solvents, as shown in Table S4.† Zeta potential values more negative than −30 mV generally represent a sufficient mutual repulsion to ensure the stability of a dispersion.[38] The zeta potential values of CR-GONRs were lower than −30 mV for several solvents, supporting the observation that dispersions of CR-GONR were sufficiently stable.

Conclusions

In summary, GONRs were prepared by unzipping MWCNTs, and CR-GONRs were prepared by adding hydrazine into homogeneous GONRs suspensions in DMF. Both GONRs and CR-GONRs had nanometre-sized hexagonal carbon domains and numerous oxygen functional groups (C/O ratio of 2.3 and 3.2 for GONRs and CR-GONRs, respectively). CR-GONRs showed complex defective structures. Stable colloidal suspensions of GONRs were obtained in hydrophilic solvents such as water, DMF, and NMP, which have high surface tensions ($\gamma > 37.10$ mJ m^{-2}) and hydrophilic properties ($\delta_p + \delta_h > 19.5$ $MPa^{1/2}$). CR-GONRs showed amphiphilic dispersion behaviours over a wide range of solvents, such as water, MeOH, EtOH, DMF, NMP, acetone, styrene, and xylene. Some solvents with an intermediate hydrophilicity ($\delta_p + \delta_h$ values between 8.8 and 13.7 $MPa^{1/2}$) resulted in poor CR-GONR dispersion stabilities.

Acknowledgements

This study was supported by the Graphene Materials/Components Development Project (10044366, Fabrication of the hybrid graphene barrier film with OTR/WVTR (10^{-6} cm^3 (g) m^{-2} per day) grade for commercialized package, photovoltaic and display technology) funded by the Ministry of Trade, industry & Energy (MI, Korea) and National Research

Foundation of Korea Grant funded by the Korean Government (MEST) (NRF-2012M1A2A2671806). This research was also supported by a grant from the Technology Development Program for Strategic Core Materials funded by the Ministry of Trade, Industry & Energy, Republic of Korea (Project No. 10050858).

Notes and references

1 P. Avouris, Z. Chen and V. Perebeinos, *Nat. Nanotechnol.*, 2007, **2**, 605–615.
2 M. F. L. De Volder, S. H. Tawfick and R. H. Baughman, *Science*, 2013, **339**, 535–539.
3 Z. Wei, D. Wang, S. Kim, S.-Y. Kim, Y. Hu, M. K. Yakes, A. R. Laracuente, Z. Dai, S. R. Marder, C. Berger, W. P. King, W. A. de Heer, P. E. Sheehan and E. Riedo, *Science*, 2010, **328**, 1373–1376.
4 S. Wang, P. K. Ang, Z. Wang, A. L. L. Tang, J. T. L. Thong and K. P. Loh, *Nano Lett.*, 2009, **10**, 92–98.
5 A. Vakil and N. Engheta, *Science*, 2011, **332**, 1291–1294.
6 M. Gullans, D. E. Chang, F. H. L. Koppens, F. J. García de Abajo and M. D. Lukin, *Phys. Rev. Lett.*, 2013, **111**, 247401.
7 A. N. Grigorenko, M. Polini and K. S. Novoselov, *Nat. Photonics*, 2012, **6**, 749–758.
8 D. N. Futaba, K. Hata, T. Yamada, T. Hiraoka, Y. Hayamizu, Y. Kakudate, O. Tanaike, H. Hatori, M. Yumura and S. Iijima, *Nat. Mater.*, 2006, **5**, 987–994.
9 M. Kaempgen, C. K. Chan, J. Ma, Y. Cui and G. Gruner, *Nano Lett.*, 2009, **9**, 1872–1876.
10 M. D. Stoller, S. Park, Y. Zhu, J. An and R. S. Ruoff, *Nano Lett.*, 2008, **8**, 3498–3502.
11 A. L. M. Reddy, A. Srivastava, S. R. Gowda, H. Gullapalli, M. Dubey and P. M. Ajayan, *ACS Nano*, 2010, **4**, 6337–6342.
12 J. Xiao, D. Mei, X. Li, W. Xu, D. Wang, G. L. Graff, W. D. Bennett, Z. Nie, L. V. Saraf, I. A. Aksay, J. Liu and J.-G. Zhang, *Nano Lett.*, 2011, **11**, 5071–5078.
13 S. Fukuzumi, H. Imahori, H. Yamada, M. E. El-Khouly, M. Fujitsuka, O. Ito and D. M. Guldi, *J. Am. Chem. Soc.*, 2001, **123**, 2571–2575.
14 W. Chen, Z. Fan, X. Pan and X. Bao, *J. Am. Chem. Soc.*, 2008, **130**, 9414–9419.
15 L. Lai, J. R. Potts, D. Zhan, L. Wang, C. K. Poh, C. Tang, H. Gong, Z. Shen, J. Linc and R. S. Ruoff, *Energy Environ. Sci.*, 2012, **5**, 7936–7942.
16 S. Stankovich, D. A. Dikin, G. H. B. Dommett, K. M. Kohlhaas, E. J. Zimney, E. A. Stach, R. D. Piner, S. T. Nguyen and R. S. Ruoff, *Nature*, 2006, **442**, 282–286.
17 W. D. Zhang, L. Shen, I. Y. Phang and T. Liu, *Macromolecules*, 2004, **37**, 256–259.
18 H. Kim, A. A. Abdala and C. W. Macosko, *Macromolecules*, 2010, **43**, 6515–6530.
19 C. Subramaniam, Y. Yasuda, S. Takeya, S. Ata, A. Nishizawa, D. Futaba, T. Yamada and K. Hata, *Nanoscale*, 2014, **6**, 2669–2674.
20 S. Ata, H. Yoon, C. Subramaniam, T. Mizuno, A. Nishizawa and K. Hata, *Polymer*, 2014, **55**, 5276–5283.
21 S. Ata, T. Mizuno, A. Nishizawa, C. Subramaniam, D. N. Futaba and K. Hata, *Sci. Rep.*, 2014, **4**, 7232.
22 Y. Huang, J. Liang and Y. Chen, *J. Mater. Chem.*, 2012, **22**, 3671–3679.
23 Y. H. Yun, V. Shanov, T. Tu, M. J. Schulz, S. Yarmolenko, S. Neralla, J. Sankar and S. Subramaniam, *Nano Lett.*, 2006, **6**, 689–693.
24 J. A. Rather and K. De wael, *Sens. Actuators, B*, 2013, **176**, 110–117.
25 W. Li, X. Geng, Y. Guo, J. Rong, Y. Gong, L. Wu, X. Zhang, P. Li, J. Xu, G. Cheng, M. Sun and L. Liu, *ACS Nano*, 2011, **5**, 6955–6961.
26 X. Li, X. Wang, L. Zhang, S. Lee and H. Dai, *Science*, 2008, **319**, 1229–1232.
27 Y.-W. Son, M. L. Cohen and S. G. Louie, *Nature*, 2006, **444**, 347–349.
28 T. B. Martins, R. H. Miwa, A. J. R. da Silva and A. Fazzio, *Phys. Rev. Lett.*, 2007, **98**, 196803.
29 D. V. Kosynkin, A. L. Higginbotham, A. Sinitskii, J. R. Lomeda, A. Dimiev, B. K. Price and J. M. Tour, *Nature*, 2009, **458**, 872–876.
30 D. Li, M. B. Müller, S. Gilje, R. B. Kaner and G. G. Wallace, *Nat. Nanotechnol.*, 2008, **3**, 101–105.
31 S. Park, J. An, I. Jung, R. D. Piner, S. J. An, X. Li, A. Velamakanni and R. S. Ruoff, *Nano Lett.*, 2009, **9**, 1593–1597.
32 S. Y. Cho, Y. S. Yun, S. Lee, D. Jang, K.-Y. Park, J. K. Kim, B. H. Kim, K. Kang, D. L. Kaplan and H.-J. Jin, *Nat. Commun.*, 2015, **6**, 7145.
33 Y. S. Yun, D.-H. Kim, S. J. Hong, M. H. Park, Y. W. Park, B. H. Kim, H.-J. Jin and K. Kang, *Nanoscale*, 2015, **7**, 15051–15058.
34 Y. S. Yun, V.-D. Le, H. Kim, S.-J. Chang, S. J. Baek, S. Park, B. H. Kim, Y.-H. Kim, K. Kang and H.-J. Jin, *J. Power Sources*, 2014, **262**, 79–85.
35 D. Bergin, V. Nicolosi, P. V. Streich, S. Giordani, Z. Sun, A. H. Windle, P. Ryan, N. P. P. Niraj, Z.-T. T. Wang, L. Carpenter, W. J. Blau, J. J. Boland, J. P. Hamilton and J. N. Coleman, *Adv. Mater.*, 2008, **20**, 1876–1881.
36 Y. Hernandez, V. Nicolosi, M. Lotya, F. M. Blighe, Z. Sun, S. De, I. T. Mcgovern, B. Holland, M. Byrne, Y. K. Gun'ko, J. J. Boland, P. Niraj, G. Duesberg, S. Krishnamurthy, R. Goodhue, J. Hutchison, V. Scardaci, A. C. Ferrari and J. N. Coleman, *Nat. Nanotechnol.*, 2008, **3**, 563–568.
37 H.-S. Kim, S. H. Yoon, S.-M. Kwon and H.-J. Jin, *Biomacromolecules*, 2009, **10**, 82–86.
38 D. Li, M. B. Müller, S. Gilje, R. B. Kaner and G. G. Wallace, *Nat. Nanotechnol.*, 2008, **3**, 101–105.